

https://doi.org/10.1070/QEL16683

Normal modes for electromagnetically induced transparency in a lambda system of degenerate energy levels

O.M. Parshkov

Abstract. **This paper presents an analytical study of the formation of normal modes of probe light for electromagnetically induced transparency in a lambda system of quantum transitions between $^3P_0$, $^3P_1^0$ and $^3P_2$ levels in the case of an elliptically polarised control field and inhomogeneous broadening. The normal modes are elliptically polarised waves with identical polarisation ellipse eccentricities but different electric vector rotation directions. The mode eccentricities are only determined by the control field polarisation ellipse eccentricity. The major axis of the polarisation ellipse of one of the normal modes is parallel to the major axis of the control light polarisation ellipse, whereas the major axis of the polarisation ellipse of the other normal mode is perpendicular to it. The former type of mode has a higher group velocity than does the latter type of mode, and both velocities depend on control light polarisation ellipse eccentricity and intensity. Probe light with an arbitrary elliptical polarisation is the sum of normal modes which propagate independently of each other. Since the modes differ in group velocity, a probe pulse entering the medium splits into two components, each of which is a normal mode. The fraction of energy in each normal mode depends only on polarisation characteristics of coupled fields and is independent of their intensity.**

Keywords: *electromagnetically induced transparency, elliptical polarisation of light, birefringence, normal modes.*

1. Introduction

The use of destructive interference of the probability amplitudes of quantum transitions between energy levels under resonant excitation of a medium by coherent laser radiation is of considerable interest both from a theoretical point of view and in the context of potential applications. Depending on the experimental configuration, such interference underlies a number of effects, the most important of which are population trapping [1, 2] and electromagnetically induced transparency (EIT) [3–5]. Restricting ourselves to EIT, note that the use of this effect is promising for producing optical quantum memory systems [4], quantum communication [4, 6, 7] and quantum information systems [3–5] and precision magnetometry [8] and chronometry [9] devices. The EIT effect underlies methods for producing high optical nonlinearity [5, 10] and amplifying light without population inversion [11]. The specifics of EIT in different situations continue to attract intense theoretical interest. For example, considerable research effort has focused on distinctive features of this effect in strongly correlated quantum gases [12], in an rf field [13], on impurities in photonic crystals [14] and in the presence of nanofibre [15].

EIT leads to a number of effects related to polarisation characteristics of coupled optical fields in the case of degenerate energy levels of quantum transitions. Wielandy and Gaeta [16] and Bo Wang et al. [17] theoretically and experimentally studied the accompanying rotation of the plane of polarisation of a probe field in response to changes in control field intensity. Agarwal and Dasgupta [18] and Sautenkov et al. [19] investigated the effect of a static magnetic field on the evolution of circular components of probe light. Linear and circular birefringence of a probe field in the case of EIT was studied theoretically and experimentally by Tai Hyun Yoon et al. [20]. In a theoretical study, Kis et al. [21] predicted the possibility of probe field propagation in the case of EIT in the form of two modes in different polarisation states.

Numerical simulation results for birefringence accompanying EIT in the field of an elliptically polarised control light were presented previously [22]. The subject of that research was a lambda system of quantum transitions between $^3P_0$, $^3P_2$ and $^3P_1^0$ degenerate energy levels of ^{208}Pb, whose vapour was used to experimentally observe EIT of circularly polarised laser fields [23, 24]. Simulation demonstrated the possibility of representing a probe field as a sum of elliptically polarised normal modes. At the same time, numerical simulation gives no way of assessing the generality of the previously obtained results [22], nor does it ensure detailed understanding of how characteristics of normal modes are related to those of coupled optical fields. The purpose of this report is to present an analytical theory of EIT, whose numerical simulation was described previously [22].

2. Governing equations

The lambda system under consideration (Fig. 1) comprises a nondegenerate lower level ($^3P_0$) and five- and threefold degenerate intermediate ($^3P_2$) and upper ($^3P_1^0$) levels of the ^{208}Pb isotope. Let ϕ_k ($k = 1, 2, \ldots, 9$) be an orthonormal basis consisting of the common eigenfunctions of the energy, squared angular momentum and angular momentum projection operators for an isolated atom that correspond to the lower ($k = 1$, $M = 0$), upper ($k = 2, 3, 4$; $M = -1, 0, 1$) and intermediate ($k = 5, 6, \ldots, 9$; $M = -2, -1, 0, 1, 2$) levels. Let D_1 and D_2 be reduced electric dipole moments of the $^3P_0 \rightarrow {}^3P_1^0$ and $^3P_2 \rightarrow {}^3P_1^0$ transitions, respectively, and ω_1 and ω_2 ($\omega_1 > \omega_2$)

O.M. Parshkov Yuri Gagarin State Technical University of Saratov, Politekhnicheskaya ul. 77, 410054 Saratov, Russia;
e-mail: oparshkov@mail.ru

Received 20 March 2018; revision received 22 August 2018
Kvantovaya Elektronika **48** (11) 1027–1034 (2018)
Translated by O.M. Tsarev

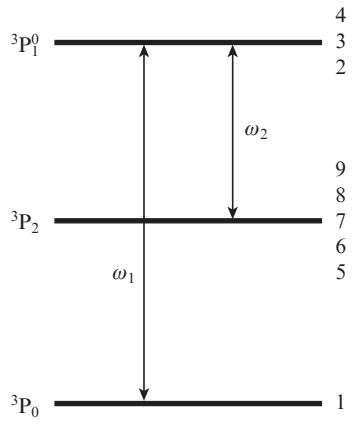

Figure 1. Lambda system of quantum transitions. Indicated on the right are the numbers of the states in the mathematical model.

be the centre frequencies of the transitions (Fig. 1). In addition, $T_1 = 1/\Delta_1$, where Δ_1 is the 1/e half width of the ω_1' frequency distribution density for the $^3P_0 \to {}^3P_1^0$ transitions as a consequence of the Doppler effect.

The total electric field of two laser pulses propagating along the z axis can be represented in the form

$$\boldsymbol{E} = \boldsymbol{E}_1 + \boldsymbol{E}_2, \tag{1}$$

where

$$\boldsymbol{E}_l = \mu_l[\boldsymbol{i}E_{xl}\cos(\omega_l t - k_l z + \delta_{xl}) + \boldsymbol{j}E_{yl}\cos(\omega_l t - k_l z + \delta_{yl})],$$

$$l = 1, 2,$$

is the electric field strength; ω_l is the carrier frequency of the probe ($l = 1$) or control ($l = 2$) field; $\mu_l = \hbar\sqrt{2l+1}/(|D_l|T_1)$; $\boldsymbol{i}$ and $\boldsymbol{j}$ are the unit vectors along the x and y axes; E_{xl} and E_{yl} are nonnegative real amplitudes; δ_{xl} and δ_{yl} are the phase shifts of the x and y components of the probe ($l = 1$) and control ($l = 2$) fields; and $k_l = \omega_l/c$. E_{xl},E_{yl}, δ_{xl} and δ_{yl} are functions of z and t.

We define f_l and g_l as

$$\begin{aligned} f_l &= [E_{xl}\exp(\mathrm{i}\delta_{xl}) - \mathrm{i}E_{yl}\exp(\mathrm{i}\delta_{yl})]/\sqrt{2}, \\ g_l &= [E_{xl}\exp(\mathrm{i}\delta_{xl}) + \mathrm{i}E_{yl}\exp(\mathrm{i}\delta_{yl})]/\sqrt{2}. \end{aligned} \tag{2}$$

Following Saleh and Teich [25], we will refer to f_l and g_l as the amplitudes of the left and right circular components of the probe ($l = 1$) and control ($l = 2$) fields. The wave function Ψ of an atom in field (1) can be represented as an expansion in terms of ϕ_k ($k = 1, 2, \ldots, 9$):

$$\Psi = \bar{c}_1\phi_1 + \left(\sum_{k=2}^{4}\bar{c}_k\phi_k\right)\exp(-\mathrm{i}\xi_1) + \left(\sum_{k=5}^{9}\bar{c}_k\phi_k\right)\exp[-\mathrm{i}(\xi_1 - \xi_2)],$$

where $\bar{c}_k$ ($k = 1, 2, \ldots, 9$) are the amplitudes of the probability that the quantum states are occupied and $\xi_l = \omega_l t - k_l z$ ($l = 1, 2$). We introduce c_i in the form

$$c_1 = p_1^*\bar{c}_1, \quad c_2 = \bar{c}_2, \quad c_4 = \bar{c}_4, \quad c_5 = p_2\bar{c}_5,$$

$$c_7 = (1/\sqrt{6})p_2\bar{c}_7, \quad c_9 = p_2\bar{c}_9,$$

where $p_l = 2D_l/|D_l|$ ($l = 1, 2$). The normalised independent variables s and w are given by

$$s = z/z_0, \quad w = (t - z/c)/T_1,$$

where $z_0 = 3\hbar c/(2\pi N|D_1|^2 T_1\omega_1)$ (N is the atomic concentration). Using the Schrödinger and Maxwell's equations, we obtain, as a first (slow envelope) approximation, the following system of equations:

$$\begin{aligned}
\frac{\partial f_1}{\partial s} &= \frac{\mathrm{i}}{\sqrt{\pi}}\int_{-\infty}^{+\infty} c_1 c_2^* \exp(-\varepsilon_1^2)\mathrm{d}\varepsilon_1, \\
\frac{\partial f_2}{\partial s} &= -\frac{\mathrm{i}}{\sqrt{\pi}}\xi\int_{-\infty}^{+\infty}(c_4^* c_9 + c_2^* c_7)\exp(-\varepsilon_1^2)\mathrm{d}\varepsilon_1, \\
\frac{\partial g_1}{\partial s} &= -\frac{\mathrm{i}}{\sqrt{\pi}}\int_{-\infty}^{+\infty} c_1 c_4^* \exp(-\varepsilon_1^2)\mathrm{d}\varepsilon_1, \\
\frac{\partial g_2}{\partial s} &= \frac{\mathrm{i}}{\sqrt{\pi}}\xi\int_{-\infty}^{+\infty}(c_2^* c_5 + c_4^* c_7)\exp(-\varepsilon_1^2)\mathrm{d}\varepsilon_1, \\
\frac{\partial c_1}{\partial w} &= -\mathrm{i}(f_1 c_2 - g_1 c_4), \\
\frac{\partial c_2}{\partial w} + \mathrm{i}\varepsilon_1 c_2 &= -\frac{\mathrm{i}}{4}(f_1^* c_1 + g_2^* c_5 - f_2^* c_7) - \gamma c_2, \\
\frac{\partial c_4}{\partial w} + \mathrm{i}\varepsilon_1 c_4 &= \frac{\mathrm{i}}{4}(g_1^* c_1 - g_2^* c_7 + f_2^* c_9) - \gamma c_4, \\
\frac{\partial c_5}{\partial w} + \mathrm{i}(\varepsilon_1 - \varepsilon_2)c_5 &= -\mathrm{i}g_2 c_2, \\
\frac{\partial c_7}{\partial w} + \mathrm{i}(\varepsilon_1 - \varepsilon_2)c_7 &= \frac{\mathrm{i}}{6}(f_2 c_2 - g_2 c_4), \\
\frac{\partial c_9}{\partial w} + \mathrm{i}(\varepsilon_1 - \varepsilon_2)c_9 &= \mathrm{i}f_2 c_4,
\end{aligned} \tag{3}$$

where $\varepsilon_1 = (\omega_1' - \omega_1)/\Delta_1$; $\varepsilon_2 = \beta\varepsilon_1$; $\xi = 0.6\beta|D_2/D_1|^2$; and $\beta = \omega_2/\omega_1$.

The system of equations (3) does not contain $\bar{c}_3$, $\bar{c}_6$ or $\bar{c}_8$, in agreement with the selection rule ($\Delta M = \pm 1$) for transitions driven by circular components of field (1). In the equations for c_2 and c_4, we phenomenologically introduced the terms $-\gamma c_2$ and $-\gamma c_4$ to take into account spontaneous decay of upper level states in the lambda system under consideration. Here $\gamma = T_1/(2\tau)$, where τ is the radiative lifetime of the $^3P_1^0$ level.

Below we use the parameters a_l, α_l and γ_l of the polarisation ellipse (PE) for probe ($l = 1$) and control ($l = 2$) light. Here a_l is the semimajor axis of the PE in units of μ_l; α_l is its angle relative to the x axis in radians; and γ_l is a compression parameter ($0 \leqslant \alpha_l < \pi$, $-1 \leqslant \gamma_l \leqslant +1$) [26]. The value of $|\gamma_l|$ determines the ratio of the minor axis to the major axis of the PE. Negative and positive values of γ_l correspond to right and left elliptical polarisations of light, respectively [25]. It is worth noting that setting a_l, α_l, γ_l and δ_{xl} values is equivalent to setting the field by (1), because it is easy to derive the following relations:

$$\begin{aligned} E_{xl} &= a_l\sqrt{[1 + \gamma_l^2 + (1 - \gamma_l^2)\cos 2\alpha_l]/2}, \\ E_{yl} &= a_l\sqrt{[1 + \gamma_l^2 - (1 - \gamma_l^2)\cos 2\alpha_l]/2}, \end{aligned} \tag{4}$$

$$\exp[\mathrm{i}(\delta_{yl}-\delta_{xl})]=\frac{(1-\gamma_l^2)\sin 2\alpha_l+2\mathrm{i}\gamma_l}{\sqrt{(1+\gamma_l^2)^2-(1-\gamma_l^2)^2\cos^2 2\alpha_l}}.$$

We assume that the probe field is so weak compared to the control field that its effect can be taken into account by the method of successive approximations with $\tilde{v}=\sqrt{E_{x1}^2+E_{y1}^2}\big/\sqrt{E_{x2}^2+E_{y2}^2}$ as a small parameter. As a zeroth approximation, we assume that $\tilde{v}=0$, i.e. that there is no probe field. Since the energy levels of quantum transitions resonant with the control field are initially unoccupied, to a zeroth approximation this field does not interact with the medium. This means that, to a zeroth approximation, the following relations are valid:

$$f_2(w,s)=f_{20}(w),\quad g_2(w,s)=g_{20}(w), \tag{5}$$

where $f_{20}(w)$ and $g_{20}(w)$ are the circular components of the control field at the input to the medium. In addition, in this approximation we have $|c_1|=2|\tilde{c}_1|=2$ and $c_i=0$ ($i=2,4,5,7,9$) because we assume that, without a probe field, only the lower energy level is occupied. Note that the circular components of the control light, as well as c_1, are identical in the zeroth and first orders of the method of successive approximations.

In what follows, we assume that $\alpha_2=0$, i.e. that the major axis of the control field PE coincides with the x axis. It then follows from (2) and (4) that

$$f_{20}(w)=\kappa_2 g_{20}(w),\quad \kappa_2=(1+\gamma_2)/(1-\gamma_2). \tag{6}$$

Taking into account these relations and taking $c_1=2$, we obtain from (3) equations for the evolution of the probe field to first order of the method of successive approximations:

$$\begin{aligned}
&\frac{\partial f_1}{\partial s}=\frac{2\mathrm{i}}{\sqrt{\pi}}\int_{-\infty}^{+\infty}c_2^*\exp(-\varepsilon_1^2)\mathrm{d}\varepsilon_1,\\
&\frac{\partial g_1}{\partial s}=-\frac{2\mathrm{i}}{\sqrt{\pi}}\int_{-\infty}^{+\infty}c_4^*\exp(-\varepsilon_1^2)\mathrm{d}\varepsilon_1,\\
&\frac{\partial c_2}{\partial w}+\mathrm{i}\varepsilon_1 c_2=-\frac{\mathrm{i}}{2}f_1^*-\frac{\mathrm{i}}{4}g_{20}^*(w)(c_5-\kappa_2 c_7)-\gamma c_2,\\
&\frac{\partial c_4}{\partial w}+\mathrm{i}\varepsilon_1 c_4=\frac{\mathrm{i}}{2}g_1^*-\frac{\mathrm{i}}{4}g_{20}^*(w)(c_7-\kappa_2 c_9)-\gamma c_4,\\
&\frac{\partial c_5}{\partial w}+\mathrm{i}(\varepsilon_1-\varepsilon_2)c_5=-\mathrm{i}g_{20}(w)c_2,\\
&\frac{\partial c_7}{\partial w}+\mathrm{i}(\varepsilon_1-\varepsilon_2)c_7=\frac{\mathrm{i}}{6}g_{20}(w)(\kappa_2 c_2-c_4),\\
&\frac{\partial c_9}{\partial w}+\mathrm{i}(\varepsilon_1-\varepsilon_2)c_9=\frac{\mathrm{i}}{6}\kappa_2 g_{20}(w)c_2.
\end{aligned} \tag{7}$$

3. Normal modes

In what follows, we assume that $|\gamma_2|\neq 1$, i.e. that the polarisation of the control field is not circular, and that

$$f_{20}(w)=f_{20},\quad g_{20}(w)=g_{20}, \tag{8}$$

where f_{20} and g_{20} are constants. Conditions (8) correspond to a counterintuitive configuration of the fields [3], which is most often used in experimental studies of EIT. Consider two probe fields with intensities $\boldsymbol{E}_1^{(1)}$ and $\boldsymbol{E}_1^{(2)}$. The field $\boldsymbol{E}_1^{(1)}$ describes an elliptically polarised probe pulse with the following parameters:

$$a_1=a_1^{(1)},\quad \alpha_1=\alpha_1^{(1)}=0,\quad \gamma_1=\gamma_1^{(1)},\quad \delta_{x1}=\delta_{x1}^{(1)}, \tag{9}$$

where $a_1^{(1)}$ depends on w and s, whereas $\gamma_1^{(1)}$ and $\delta_{x1}^{(1)}$ are constants. This pulse will be referred to as a parallel mode, because the major axis of its PE is parallel to the major axis of the control field PE. The field $\boldsymbol{E}_1^{(2)}$ describes an elliptically polarised probe pulse with

$$a_1=a_1^{(2)},\ \alpha_1=\alpha_1^{(2)}=\pi/2,\ \gamma_1=\gamma_1^{(2)}=-\gamma_1^{(1)},\ \delta_{x1}=\delta_{x1}^{(2)}. \tag{10}$$

Note that $a_1^{(2)}$ depends on w and s, whereas $\gamma_1^{(2)}$ and $\delta_{x1}^{(2)}$ are constants. This pulse will be referred to as a perpendicular mode, because the major axis of its PE is perpendicular to the major axis of the control field PE. If $f_1^{(i)}$ and $g_1^{(i)}$ are complex amplitudes of the left-hand (σ_-) and right-hand (σ_+) polarised circular components of the parallel ($i=1$) and perpendicular ($i=2$) modes, we obtain using (2) and (4)

$$f_1^{(1)}=\kappa g_1^{(1)},\quad f_1^{(2)}=-\frac{1}{\kappa}g_1^{(2)},\quad \kappa=\frac{1+\gamma_1^{(1)}}{1-\gamma_1^{(1)}}. \tag{11}$$

It is easy to show that the Jones vectors [25] of the parallel and perpendicular modes are mutually orthogonal and that, hence, the probe field strength $\boldsymbol{E}_1$ can be represented in the form $\boldsymbol{E}_1=\boldsymbol{E}_1^{(1)}+\boldsymbol{E}_1^{(2)}$. Taking into account this and (11), we obtain

$$f_1=\kappa g_1^{(1)}-(1/\kappa)g_1^{(2)},\quad g_1=g_1^{(1)}+g_1^{(2)}.$$

Let κ [third equality in (11)] be given by

$$\kappa=-p+\sqrt{p^2+1}, \tag{12}$$

where $p=10\gamma_2/(1-\gamma_2^2)$.

Combining Eqns (7), we find that the evolution of $g_1^{(1)}$ can be described by the system of equations (see Appendix 1)

$$\begin{aligned}
&\frac{\partial g_1^{(1)}}{\partial s}=\frac{2\mathrm{i}}{\sqrt{\pi}}\,\frac{1}{\kappa^2+1}\int_{-\infty}^{+\infty}U_1^*\exp(-\varepsilon_1^2)\mathrm{d}\varepsilon_1,\\
&\frac{\partial U_1}{\partial w}+\mathrm{i}\varepsilon_1 U_1=-\frac{\mathrm{i}}{2}(1+\kappa^2)g_1^{(1)*}-\frac{\mathrm{i}}{4}g_2^* V_1-\gamma U_1,\\
&\frac{\partial V_1}{\partial w}+\mathrm{i}(\varepsilon_1-\varepsilon_2)V_1=-\mathrm{i}g_2 q_1 U_1.
\end{aligned} \tag{13}$$

U_1, V_1 and q_1 in (13) are given by

$$\begin{aligned}
&U_1=\kappa c_2-c_4,\quad V_1=\kappa c_5-(\kappa_2\kappa+1)c_7+\kappa_2 c_9,\\
&q_1=1+\kappa_2[\kappa_2+(1/\kappa)]/6.
\end{aligned} \tag{14}$$

In a similar way, we find that the evolution of $g_1^{(2)}$ is described by the system of equations

$$\frac{\partial g_1^{(2)}}{\partial s}=-\frac{2\mathrm{i}}{\sqrt{\pi}}\,\frac{\kappa^2}{\kappa^2+1}\int_{-\infty}^{+\infty}U_2^*\exp(-\varepsilon_1^2)\mathrm{d}\varepsilon_1,$$

$$\frac{\partial U_2}{\partial w} + \mathrm{i}\varepsilon_1 U_2 = \frac{\mathrm{i}}{2}\frac{\kappa^2+1}{\kappa^2} g_1^{(2)*} - \frac{\mathrm{i}}{4} g_2^* V_2 - \gamma U_2, \qquad (15)$$

$$\frac{\partial V_2}{\partial w} + \mathrm{i}(\varepsilon_1 - \varepsilon_2) V_2 = -\mathrm{i} g_2 q_2 U_2,$$

where

$$U_2 = (1/\kappa)c_2 + c_4; \quad V_2 = (1/\kappa)c_5 - (\kappa_2/\kappa - 1)c_7 - \kappa_2 c_9; \qquad (16)$$
$$q_2 = 1 + \kappa_2(\kappa_2 - \kappa)/6.$$

The systems of equations (13) and (15) have no common dependent variables and, hence, can be solved independently of each other. This means that, if condition (12) is satisfied, the parallel and perpendicular modes of the probe field propagate in the medium independently of each other as well. Moreover, according to (9) and (10) the polarisation characteristics of these modes remain unchanged. The above leads us to conclude that the perpendicular and parallel modes are elliptically polarised normal modes of the probe light.

Taking into account (12) and the definition of κ [see (11)], we can find the compression parameter of the PE of the parallel normal mode, $\gamma_1^{(1)}$, as a function of the compression parameter of the control field PE, γ_2 (Fig. 2). It is seen that $\gamma_1^{(1)}$ is of opposite sign to γ_2 and that $\gamma_1^{(1)}$ is an odd function of γ_2. At $\gamma_2 = 0$, we have $\gamma_1^{(1)} = \gamma_1^{(2)} = 0$, i.e. in the case of linear polarisation of the control field both normal modes are linearly polarised. If $|\gamma_2|$ approaches unity, $|\gamma_1^{(1)}|$ also approaches unity. Therefore, if the probe field is circularly polarised, so are both of its normal modes.

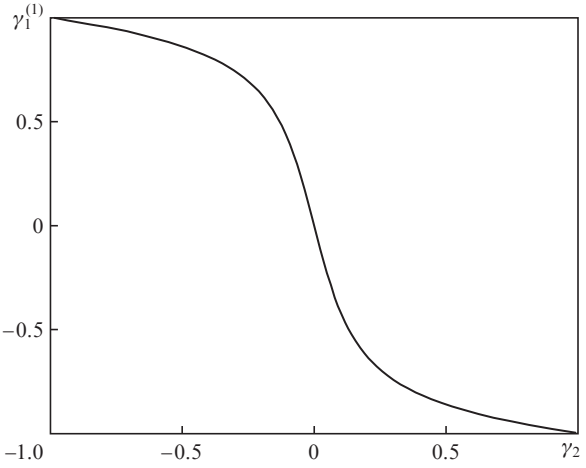

Figure 2. Graph of $\gamma_1^{(1)}$ against γ_2.

Assume that, on the input surface of the medium ($s = 0$), the probe field has the form of an elliptically polarised pulse with a polarisation state constant in time. First, consider the case of $\gamma_2 \neq 0$. We denote the values of a_1, α_1, γ_1 and δ_{x1} on the input surface as $a_{10}, \alpha_{10}, \gamma_{10}$ and δ_{x10}. Among these parameters, only a_{10} is assumed to depend on time w. Since the input probe field is not phase-modulated, we can take $\delta_{x10} = 0$ without loss of generality. Let $a_{10}^{(i)}, \alpha_1^{(i)}, \gamma_1^{(i)}$ and $\delta_{x1}^{(i)}$ ($i = 1, 2$) be the values of $a_1^{(i)}, \alpha_1^{(i)}, \gamma_1^{(i)}$ and $\delta_{x1}^{(i)}$ on the input surface. According to (9) and (10), $\alpha_1^{(1)} = 0$ and $\alpha_1^{(2)} = \pi/2$, whereas $\gamma_1^{(1)}$ and $\gamma_1^{(2)}$ can be found as described above. The values of $a_{10}^{(i)}$ and $\delta_{x1}^{(i)}$ are to be determined.

Let us introduce A, B and C – parameters independent of w and s:

$$A = \varepsilon_+(\alpha_{10}, \gamma_{10}), \quad B = \mathrm{sign}(\gamma_2)\varepsilon_-(\alpha_{10}, \gamma_{10})\cos\delta_{y10}, \qquad (17)$$
$$C = -\mathrm{sign}(\gamma_2)\varepsilon_-(\alpha_{10}, \gamma_{10})\sin\delta_{y10},$$

where

$$\varepsilon_\pm(\alpha_{10}, \gamma_{10}) = \sqrt{[1 + \gamma_{10}^2 \pm (1 - \gamma_{10}^2)\cos 2\alpha_{10}]/2};$$

$$\exp(\mathrm{i}\delta_{y10}) = \frac{(1 - \gamma_{10}^2)\sin 2\alpha_{10} + 2\mathrm{i}\gamma_{10}}{\sqrt{(1 + \gamma_{10}^2)^2 - (1 - \gamma_{10}^2)^2\cos^2 2\alpha_{10}}};$$

and $\mathrm{sign}(x)$ is the sign function. Let X, Y, Z and T be given by

$$X = \frac{A + |\gamma_1^{(1)}|C}{1 + (\gamma_1^{(1)})^2}, \quad Y = \frac{|\gamma_1^{(1)}|B}{1 + (\gamma_1^{(1)})^2}, \quad Z = \frac{|\gamma_1^{(1)}|A - C}{1 + (\gamma_1^{(1)})^2}, \qquad (18)$$
$$T = -\frac{B}{1 + (\gamma_1^{(1)})^2}.$$

The missing characteristics $a_{10}^{(i)}$ and $\delta_{x1}^{(i)}$ ($i = 1, 2$) of the normal modes on the input surface of the medium are then given by (see Appendix 2)

$$a_{10}^{(1)} = a_{10}\sqrt{X^2 + Y^2}, \qquad a_{10}^{(2)} = a_{10}\sqrt{Z^2 + T^2},$$
$$\cos\delta_{x1}^{(1)} = X/\sqrt{X^2 + Y^2}, \quad \sin\delta_{x1}^{(1)} = Y/\sqrt{X^2 + Y^2}, \qquad (19)$$
$$\cos\delta_{x1}^{(2)} = Z/\sqrt{Z^2 + T^2}, \quad \sin\delta_{x1}^{(2)} = T/\sqrt{Z^2 + T^2}.$$

According to (19), the $a_{10}^{(i)}(w)$ ($i = 1, 2$) functions are proportional to $a_{10}(w)$. In other words, the variation of the major axes of the PEs of the normal modes on the input surface with time w is similar to the time variation of the major axis of the PE of an input probe pulse. In the case of circularly polarised input probe light, the α_{10} angle is not defined, but relations (19) remain valid at any α_{10}.

At $\gamma_2 = 0$, the expressions for $a_{10}^{(i)}$ and $\delta_{x1}^{(i)}$ ($i = 1, 2$) through input probe pulse parameters have the form

$$a_{10}^{(1)} = a_{10}|\cos\alpha_{10}|, \quad \delta_{x1}^{(1)} = 0, \quad a_{10}^{(2)} = a_{10}\sin\alpha_{10},$$
$$\delta_{x1}^{(2)} = 0 \text{ for } 0 \leqslant \alpha_{10} \leqslant \pi/2, \qquad (20)$$
$$a_{10}^{(1)} = a_{10}|\cos\alpha_{10}|, \quad \delta_{x1}^{(1)} = 0, \quad a_{10}^{(2)} = a_{10}\sin\alpha_{10},$$
$$\delta_{x1}^{(2)} = \pi \text{ for } \pi/2 < \alpha_{10} < \pi.$$

The propagation of probe light in a medium can be thought of as the propagation of two independent normal modes. Characteristics of such modes on the input surface can then be determined using (19) or (20) from known characteristics of input probe light. If an input probe field has the form of a sufficiently short pulse, a_{10} differs significantly from zero only in some time interval w. According to (19) and (20), $a_{10}^{(1)}$ and $a_{10}^{(2)}$ will also have such properties and, hence, each normal mode in a medium will have the form of a pulse. While propagating, a pulse corresponding to each normal mode becomes distorted and decays. In the case of EIT, however, these factors

show up rather slowly as the distance passed by a pulse in the medium increases. This allows us to approximately estimate energetic characteristics and propagation group velocities of normal mode pulses.

Let $I_{10}^{(1)}$ and $I_{10}^{(2)}$ be the intensities of the perpendicular and parallel normal modes, respectively, on the input surface. Then, we have

$$I_{10}^{(2)}/I_{10}^{(1)} = (a_{10}^{(2)}/a_{10}^{(1)})^2. \tag{21}$$

The parameters $a_{10}^{(1)}$ and $a_{10}^{(2)}$ can, in turn, be expressed through the polarisation characteristics α_{10} and γ_{10} of an input probe pulse using (19) and (20). Formula (21) can be used to approximately estimate the intensity ratio of normal modes in a medium.

The ratio of pulse energies of normal modes in a medium is determined by two factors. One of them is the ratio of pulse energies on the input surface of the medium. This ratio coincides with the pulse intensity ratio (because $a_{10}^{(2)}/a_{10}^{(1)}$ is time-independent) and, according to (19) and (20), depends only on γ_2, α_{10} and γ_{10}. Figure 3 shows contour lines of the function $R(\alpha_{10},\gamma_{10},\gamma_1)$ – the fraction of the input probe pulse energy in the parallel mode on the input surface – at $\alpha_{10} = \pi/6$. According to Fig. 3, this fraction exceeds 0.5 if γ_{10} and γ_1 have opposite signs.

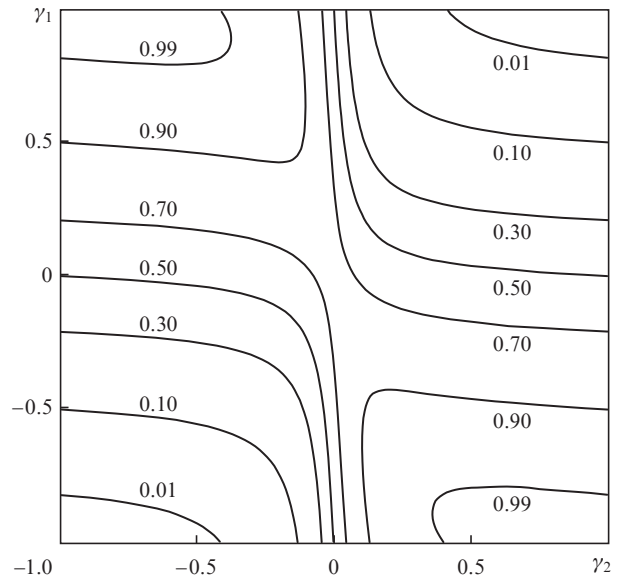

Figure 3. Contour lines of the function $R(\alpha_{10},\gamma_{10},\gamma_1)$ at $\alpha_{10} = \pi/6$.

The other factor is the difference in the rate of energy absorption by the medium between the normal modes. According to the general theory of EIT [1], the energy of a slower propagating pulse of the perpendicular mode (see below) would be expected to decrease faster than that of a pulse of the parallel mode.

Let $V_1^{(i)}$ be the group velocity of a pulse of the parallel ($i = 1$) and perpendicular ($i = 2$) normal modes in the s, w frame of reference. It can be shown (Appendix 3) that

$$V_1^{(i)} = (1/4)|g_2|^2 q_i \ (i = 1, 2), \tag{22}$$

where q_i are determined by the last equalities in (14) and (16).

Formula (22) can be written in the form

$$V_1^{(i)} = \left(\frac{1}{8}\right) I_2 \frac{(1-\gamma_2)^2}{1+\gamma_2^2} q_i \ \ (i = 1, 2),$$

where I_2 is the control light intensity in units of μ_2^2. This means that the group velocities of the modes decrease with decreasing control light intensity. This is consistent with the conclusion drawn from EIT theory [1] as to how the velocity of probe field pulses depends on control light intensity. Figure 4 shows graphs of $V_1^{(i)}/I_2$ against γ_2. It is seen that the parallel mode always has a higher group velocity than does the perpendicular mode. Note that, at a constant value of I_2, the difference between the velocities of the normal modes is smallest in the case of linearly polarised control light and rises monotonically as the control field approaches circular polarisation. Moreover, it follows from Fig. 4 that $V_1^{(i)}$ (i = 1, 2) are odd functions of γ^2.

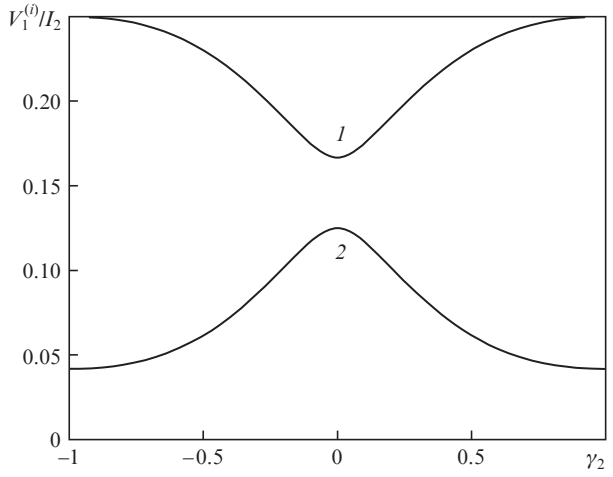

Figure 4. Graphs of (*1*) $V_1^{(1)}/I_2$ and (*2*) $V_1^{(2)}/I_2$ against γ_2.

4. Normal modes: comparison of analytical and numerical results

A previous report [22] presented results of numerically solving the system of equations (3) subject to boundary conditions corresponding to the possibility of formation of normal modes of a probe field. Let us compare those results with analytical theory predictions. In the first calculation in Ref. [22], boundary conditions describing the probe and control fields on the input surface ($s = 0$) were taken in the form

$$\alpha_{10} = \pi/6, \quad a_{10} = 0.2\mathrm{sech}[(w - 20)/5], \tag{23}$$

$$\gamma_{10} = -0.5, \quad \delta_{x10} = 0,$$

$$\alpha_{20} = 0, \quad a_{20} = 6.6516, \quad \gamma_{20} = -0.3, \quad \delta_{x20} = 0. \tag{24}$$

The initial conditions ($w = 0$) corresponded to all ^{208}Pb atoms being at the lower energy level.

Conditions (23) describe an input probe light pulse of 1.5 ns duration with a peak intensity of 65 W cm^{-2}. According to (24), the constant control light intensity is approximately 20 kW cm^{-2}. Since the peak intensity of the input probe pulse is more than a factor of 300 lower than the control field

intensity, described by formulas (23) and (24), we deal with a weak probe field. (The choice of resonance medium and input light parameters was substantiated in a previous study [22].)

The calculation results are presented in Figs 5a–5c. The dependences of the probe light intensity I_1 (in units of μ_1^2) on w at different constant distances s are represented in Figs 5a–5c by thick solid lines. It is seen that, at sufficiently small distances in the medium, the probe light pulse begins to separate into two components (Fig. 5b, pulses *1*, *2*). The shape of the curves describing the evolution of α_1 and γ_1 suggests that, as the probe field passes through a given point, the angle α_1 gradually varies from zero to $\sim\pi/2$, whereas γ_1 gradually decreases from $\sim$0.74 to near –0.74.

At sufficiently large distances, the probe pulse energy turns out to be concentrated in two pulses (Fig. 5c, pulses *1*, *2*). In the localisation region of each pulse, the polarisation characteristics of the light remain unchanged in both space and time. Our calculations give $\alpha_1 = 0$ and $\gamma_1 = 0.7415$ for pulse *1* and $\alpha_1 = \pi/2$ and $\gamma_1 = -0.7418$ for pulse *2*.

Using (12) and the third formula in (11), we find the $\gamma_1^{(1)} = 0.7414$ and $\gamma_1^{(2)} = -0.7414$ predicted analytically. This agrees well with the γ_1 values obtained above for pulses *1* and *2* in Fig. 5c, respectively.

Using the $\gamma_1^{(1)}$ and $\gamma_1^{(2)}$ values thus found and (19), we find all characteristics of the parallel and perpendicular normal modes that constitute the input probe field [22]:

$$\alpha_1^{(1)} = 0, \quad a_{10}^{(1)} = 0.0720\,\mathrm{sech}[(w-20)/5],$$
$$\gamma_1^{(1)} = 0.7414, \quad \delta_{x1}^{(1)} = -0.4991, \tag{25}$$

$$\alpha_1^{(2)} = \pi/2, \quad a_{10}^{(2)} = 0.1646\,\mathrm{sech}[(w-20)/5],$$
$$\gamma_1^{(2)} = -0.7414, \quad \delta_{x1}^{(2)} = 0.2865. \tag{26}$$

The evolution of the parallel normal mode in a medium was studied by numerically solving the system of equations (3) subject to the boundary conditions (24) and (25). Similarly, using the boundary conditions (24) and (26), we studied the behaviour of the perpendicular normal mode in a medium. Our calculations show that both modes propagate in the medium without changes in their polarisation characteristic $\alpha_1^{(i)}$ or $\gamma_1^{(i)}$ or phases $\delta_{x1}^{(i)}$ (i = 1, 2), which were assumed to remain unchanged in going from Eqn (3) to (13) and (15).

Figures 5d–5f show the variations of the intensities of the parallel (solid lines) and perpendicular (dashed lines) normal modes with time w at the same distances s as in Figs 5a–5c. At each distance and each time, the sum of the intensities of the normal modes (Figs 5d–5f) coincides with the total probe field intensity in the medium to within 0.3% (Figs 5a–5c). Thus, numerical analysis based on the solution to the input equation (3) supports the conclusion that a probe field in a medium can be represented as the sum of normal modes.

The numerical solution to system (3) shows that, at a distance s = 400, the intensity ratio of the perpendicular and parallel modes is 4, whereas an estimate using formula (21) gives an intensity ratio of 5.2. Moreover, numerically solving system (3) we obtained group velocities of the parallel and perpendicular modes $V_1^{(1)} = 9.4$ and $V_1^{(2)} = 3.7$, respectively. Estimates by formulas (22) yield $V_1^{(1)} = 9.9$ and $V_1^{(2)} = 4.1$. The cause of the discrepancy between the intensities and velocities of the normal modes evaluated by formulas (21) and (22) of analytical theory and by numerically solving system (3) is that, in deriving these formulas, the distortion and decay of probe field pulses in the medium were left out of consideration. Note that these factors are more important in the evolution of the perpendicular normal mode. Because of this, the deviations of the values obtained by formulas (21) and (22) from those evaluated by numerically solving system (3) are larger in the case of the perpendicular normal mode than in the case of the parallel normal mode.

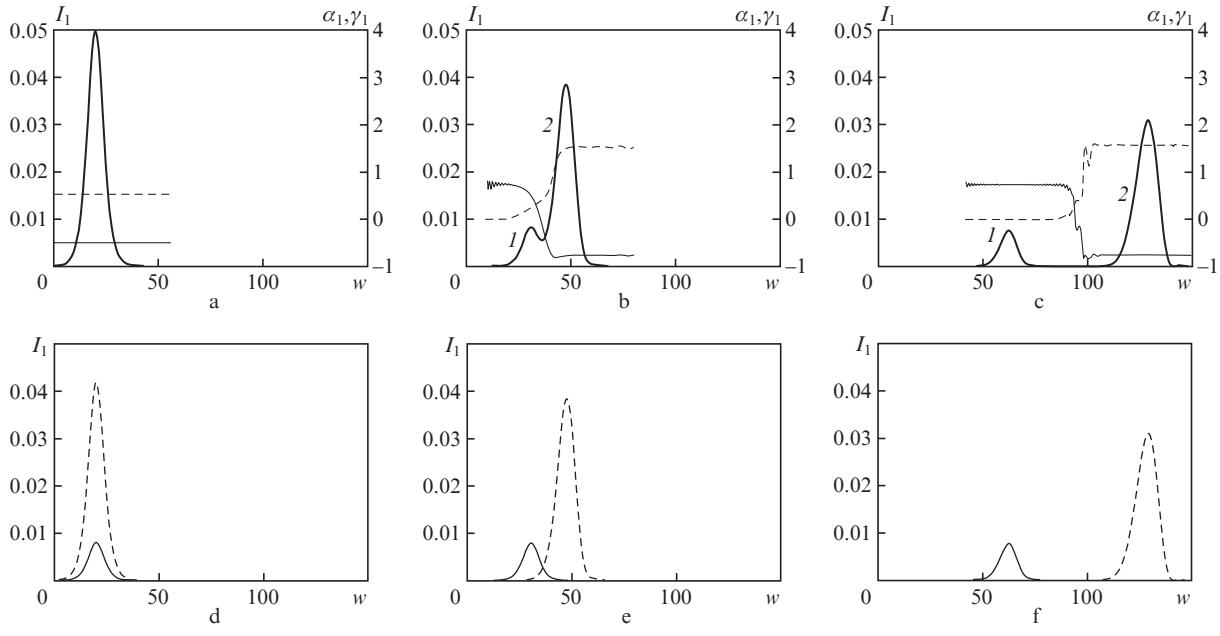

Figure 5. Evolution of probe field characteristics in a medium at s = (a) 0, (b) 100 and (c) 400 (I_1 is represented by thick solid lines; α_1, by dashed lines; and γ_1, by thin solid lines) and the intensity of the longitudinal (solid lines) and perpendicular (dashed lines) normal modes at s = (d) 0, (e) 100 and (f) 400.

Additional numerical results obtained at different parameters of input probe and control fields and the corresponding dimensional estimates were presented in a previous report [22].

5. Conclusions

Analytical treatment confirms the conclusion derived from numerical analysis [22] that, in the case of EIT in a lambda system of degenerate quantum transitions and an elliptically polarised control field, an isotropic medium can become birefringent, with elliptically polarised normal modes of a probe field. Note that birefringence with such normal modes originates from the propagation of radio waves in magnetised cosmic plasma [27]. The major axis of the PE of one of the normal modes is parallel to the major axis of the PE of control light, whereas the major axis of the PE of the other normal mode is perpendicular to it. The electric vectors of the normal modes have opposite rotation directions. Moreover, the rotation direction of the former type of mode is opposite to that of the control field. The PEs of the two modes have identical eccentricities.

It has been shown analytically that a sufficiently weak probe field can be represented as the sum of normal modes which propagate in the medium independently of each other. The former type of mode (parallel mode) has been shown to have a higher group velocity than does the latter type of mode (perpendicular mode). In connection with this, at a sufficiently large distance from the input surface, the probe field energy is concentrated in two individual pulses. In the initial stage of a probe pulse decay, the pulse of the former type of normal mode has higher intensity than does the latter type of mode if the electric vectors of the input probe pulse and control pulse have opposite rotation directions. At identical rotation directions, the latter type of normal mode has a higher pulse intensity. In all cases, propagating in a medium the former type of normal mode decays less than the latter type.

Note that steady-state EIT without inhomogeneous broadening, with the same set of energy levels as in our case, was studied theoretically by Kis et al. [21]. However, they considered a high-frequency field as a strong control field [21] and showed that, in such a case, normal modes can also exist, but only one of them is involved in probe field energy transfer, whereas the other experiences a strong attenuation.

Appendix 1

Equations (13) follow from the system of equations (7) if the condition

$$1 + \kappa_2[\kappa_2 + (1/\kappa)]/6 = \kappa^2 + \kappa[\kappa_2 + (1/\kappa)]/6. \tag{A1.1}$$

is satisfied. Equations (15) follow from the system of equations (7) if the condition

$$1 + \kappa_2(\kappa_2 - \kappa)/6 = \kappa_2^2 - (\kappa_2 - \kappa)/(6\kappa). \tag{A1.2}$$

is satisfied. From definitions (6) and (11) of κ and κ_2, we conclude that Eqns (A1.1) and (A1.2) are equivalent to one equation,

$$\kappa^2 + 2p\kappa - 1 = 0, \tag{A1.3}$$

where p is given by the formula after (12). According to (11), κ is nonnegative. The nonnegative root of (A1.3) is given by (12). Therefore, if (12) is satisfied the system of equations splits into two independent systems: (13) and (15).

Appendix 2

The J_{x0} and J_{y0} components of the Jones vector [26] of probe light on the $s = 0$ input surface at $\delta_{x10} = 0$ are given by

$$J_{x0} = \mu_1 a_{10}\varepsilon_+(\alpha_{10},\gamma_{10}), \quad J_{y0} = \mu_1 a_{10}\varepsilon_-(\alpha_{10},\gamma_{10})\exp(\mathrm{i}\delta_{y10}).$$

The $J_{x0}^{(i)}$ and $J_{y0}^{(i)}$ components of the Jones vector of the parallel ($i = 1$) and perpendicular ($i = 2$) modes on the input surface have the form

$$\begin{aligned} J_{x0}^{(1)} &= \mu_1 a_{10}^{(1)}\exp(\mathrm{i}\delta_{x1}^{(1)}), \\ J_{y0}^{(1)} &= \mu_1 \left|\gamma_1^{(1)}\right| a_{10}^{(1)}\exp[\mathrm{i}(\delta_{x1}^{(1)} - \mathrm{sign}(\gamma_2)\pi/2)], \\ J_{x0}^{(2)} &= \mu_1 \left|\gamma_1^{(1)}\right| a_{10}^{(2)}\exp(\mathrm{i}\delta_{x1}^{(2)}), \\ J_{y0}^{(2)} &= \mu_1 a_{10}^{(2)}\exp[\mathrm{i}(\delta_{x1}^{(2)} + \mathrm{sign}(\gamma_2)\pi/2)]. \end{aligned} \tag{A2.1}$$

We use the equalities

$$J_{x0} = J_{x0}^{(1)} + J_{x0}^{(2)}, \quad J_{y0} = J_{y0}^{(1)} + J_{y0}^{(2)} \tag{A2.2}$$

and substitute relations (A2.1) into them. Assuming that $\gamma_2 \neq 0$, we multiply both sides of the latter equality in (A2.2) by $\mathrm{i}\,\mathrm{sign}\gamma_2 \neq 0$, separate the real and imaginary parts of the equations obtained and introduce X, Y, Z and T unknowns:

$$\begin{aligned} X &= (a_{10}^{(1)}/a_{10})\cos\delta_{x1}^{(1)}, \quad Y = (a_{10}^{(1)}/a_{10})\sin\delta_{x1}^{(1)}, \\ Z &= (a_{10}^{(2)}/a_{10})\cos\delta_{x1}^{(2)}, \quad T = (a_{10}^{(2)}/a_{10})\sin\delta_{x1}^{(2)}. \end{aligned} \tag{A2.3}$$

As a result, we obtain the following system of linear algebraic equations:

$$\begin{aligned} &X + \left|\gamma_1^{(1)}\right| Z = A, \quad Y + \left|\gamma_1^{(1)}\right| T = 0, \\ &\left|\gamma_1^{(1)}\right| Y - T = B, \quad \left|\gamma_1^{(1)}\right| X - Z = C, \end{aligned}$$

where A, B and C are given by (17). The solution to this system is given by formulas (18). Comparing (18) and (A2.3), we obtain (19). At $\gamma_2 = 0$ and, accordingly, $\gamma_1^{(1)} = 0$, Eqns (20) directly follow from Eqns (A2.2).

Appendix 3

It follows from (2) and (4) that, in the case of the parallel normal mode, the condition

$$g_1^{(1)} = (1/\sqrt{2})a_1^{(1)}(1 - \gamma_1^{(1)})\exp(\mathrm{i}\delta_{x1}^{(1)}).$$

is satisfied. We introduce new dependent variables,

$$P_1 = \mathrm{i}\frac{\exp(-\mathrm{i}\delta_{x1}^{(1)})}{(\kappa^2 + 1)}U_1^*, \quad Q_1 = \mathrm{i}\frac{\exp(-\mathrm{i}\delta_{x1}^{(1)})}{(\kappa^2 + 1)}V_1^*,$$

and neglect relaxation processes and the inhomogeneous broadening of lines due to quantum transitions. System (13) then transforms into a system of equations that describes the spatiotemporal evolution of the major axis of the PE of the parallel normal mode field in a medium:

$$\frac{\partial a_1^{(1)}}{\partial s} = \frac{2\sqrt{2}}{1-\gamma_1^{(1)}} P_1, \quad \frac{\partial P_1}{\partial w} = \frac{\gamma_1^{(1)}-1}{2\sqrt{2}} a_1^{(1)} + \frac{\mathrm{i}}{4} g_2 Q_1,$$
$$\frac{\partial Q_1}{\partial w} = \mathrm{i} g_2^* q_1 P_1. \tag{A3.1}$$

Let us transform to new independent variables,

$$u = s - V_1^{(1)} w, \quad v = s,$$

where $V_1^{(1)}$ is the group velocity of a parallel normal mode pulse in the s, w frame of reference. Assuming the distortion of the parallel mode envelope $a_1^{(1)}$ to be sufficiently slow, we take

$$a_1^{(1)} = \bar{a}_1^{(1)}(u) + \tilde{a}_1^{(1)}(u,v), \quad P_1 = \bar{P}_1(u) + \tilde{P}_1(u,v),$$
$$Q_1 = \bar{Q}_1(u) + \tilde{Q}_1(u,v).$$

Here $\tilde{a}_1^{(1)}$, $\tilde{P}_1$ and $\tilde{Q}_1$ are small corrections whose effect can be taken into account by the method of successive approximations. As a zeroth approximation of this method, the system of equations (A3.1) then takes the form

$$\frac{\mathrm{d}\bar{a}_1^{(1)}}{\mathrm{d}u} = \frac{2\sqrt{2}}{1-\gamma_1^{(1)}} \bar{P}_1, \quad V_1^{(1)} \frac{\mathrm{d}\bar{P}_1}{\mathrm{d}u} = \frac{1-\gamma_1^{(1)}}{2\sqrt{2}} \bar{a}_1^{(1)} - \frac{\mathrm{i}}{4} g_2 \bar{Q}_1,$$
$$V_1^{(1)} \frac{\mathrm{d}\bar{Q}_1}{\mathrm{d}u} - \mathrm{i} g_2^* q_1 \bar{P}_1, \tag{A3.2}$$

where q_1 is given by the last formula in (14). From the system of equations (A3.2), we obtain an equation describing the evolution of $\bar{P}_1(u)$:

$$\frac{\mathrm{d}^2 \bar{P}_1}{\mathrm{d}u^2} = \frac{1}{V_1^{(1)}} \left(1 - \frac{|g_2|^2 q_1}{4 V_1^{(1)}} \right) \bar{P}_1. \tag{A3.3}$$

$V_1^{(1)}$ is nonnegative by definition. Let κ^2 denote the coefficient of $\bar{P}_1$ on the right hand side of Eqn (A3.3). If the condition $\kappa^2 = 0$ is not satisfied, $\bar{P}_1$ can be expressed linearly through exponential functions of a real or purely imaginary argument. According to the first equation in (A3.2), this in turn means that the function $\bar{a}_1^{(1)}(u)$ does not tend to zero as $|u|$ tends to infinity and that the field described by it is not a pulse. Using the condition $\kappa^2 = 0$, we can determine the group velocity $V_1^{(1)}$. In a similar way, we find the group velocity of the perpendicular normal mode, $V_1^{(2)}$. As a result, we obtain equalities (22).

References

1. Agap'ev B.D., Gornyi M.B., Matisov B.G., Rozhdestvenskii Yu.V. *Usp. Fiz. Nauk*, **163**, 1 (1993).
2. Vitanov N.V., Rangelov A.A., Shore B.W., Bergmann K. *Rev. Mod. Phys.*, **89**, 015006 (2017).
3. Harris S.E. *Phys. Today*, **50**, 36 (1997).
4. Lukin M.D. *Rev. Mod. Phys.*, **75**, 457 (2003).
5. Fleischhauer M., Imamoğlu A., Marangos J.P. *Rev. Mod. Phys.*, **77**, 633 (2005).
6. Duan L.-M., Lukin M.D., Cirac J.I., Zoller P. *Nature (London)*, **414**, 413 (2001).
7. Sinatra A. *Phys. Rev. Lett.*, **97**, 253601 (2006).
8. Martinelli M., Valente P., Failache H., Felinto D., Cruz L.S., Nussenzveig P., Lezama A. *Phys. Rev. A*, **69**, 043809 (2004).
9. Godone A., Micallilizio S., Levi F. *Phys. Rev. A*, **66**, 063807 (2002).
10. Lukin M.D., Imamoğlu A. *Nature (London)*, **413**, 273 (2001).
11. Kocharovskaya O., Mandel P. *Phys. Rev. A*, **42**, 523 (1990).
12. Jen H.H., Daw-Wei Wang. *Phys. Rev. A*, **87**, 061802(R) (2013).
13. Basler C., Grzesiak J., Helm H. *Phys. Rev. A*, **92**, 013809 (2015).
14. Ronggang Liu, Tong Liu, Yingying Wang, Yujie Li, Bingzheng Gai. *Phys. Rev. A*, **96**, 053823 (2017).
15. Fam Le Kien, Rauschenbeutel A. *Phys. Rev. A*, **91**, 053847 (2015).
16. Wielandy S., Gaeta A.L. *Phys Rev. Lett.*, **81**, 3359 (1998).
17. Bo Wang, Shujing Li, Jie Ma, Hai Wang, Peng K.C., Min Xiao. *Phys. Rev. A*, **73**, 051801(R) (2006).
18. Agarwal G.S., Shubhrangshu Dasgupta. *Phys. Rev. A*, **67**, 023814 (2003).
19. Sautenkov V.A., Rostovtsev Y.V., Chen H., Hsu P., Agarwal G.S., Scully M.O. *Phys. Rev. Lett.*, **94**, 233601 (2005).
20. Tai Hyun Yoon, Chang Yong Park, Sung Jong Park. *Phys. Rev. A*, **70**, 061803(R) (2004).
21. Kis Z., Demeter G., Janszky J. *J. Opt. Soc. Am. B*, **30**, 829 (2013).
22. Parshkov O.M. *Quantum Electron.*, **47** (10), 892 (2017) [*Kvantovaya Elektron.*, **47** (10), 892 (2017)].
23. Maneesh Jain, Kasapi A., Yin G.Y. *Phys. Rev. Lett.*, **75**, 4385 (1995).
24. Kasapi A., Maneesh Jain, Yin G.Y., Harris S.E. *Phys. Rev. Lett.*, **74**, 2447 (1995).
25. Saleh B.E.A., Teich M.C. *Fundamentals of Photonics* (New York: Wiley–Interscience, 2007; Dolgoprudnyi: Izdatel'skii Dom Intellekt, 2012) vol. 1.
26. Born M., Wolf E. *Principles of Optics* (Oxford: Pergamon, 1969; Moscow: Nauka, 1970).
27. Longair M.S. *High Energy Astrophysics* (Cambridge: Cambridge Univ. Press, 1981; Moscow: Mir, 1983).